

# A QoE-aware Reinforcement Approach to Disseminate Warning Videos on LTE-VANETs

Carlos Quadros<sup>1</sup>, Aldri Santos<sup>2</sup>, Denis Rosário<sup>1</sup>, Eduardo Cerqueira<sup>1</sup>

<sup>1</sup>Faculty of Computer Engineering and Telecommunication – UFPA

<sup>2</sup>Wireless and Advanced Networks (NR2) - Dept. of Informatics – UFPR

{quadros, denis, cerqueira}@ufpa.br, aldri@ufpr.br,

**Abstract.** *The wide range of Vehicular Ad-hoc NETWORK's (VANETs) applications, e.g., real-time video dissemination, have made VANETs an interesting field of mobile wireless communication. Vehicle-to-Vehicle (V2V) communication enables users to distribute significant amount of real-time video traffic over VANETs and to alleviate congestion over LTE networks. However, the video delivery process considering an adequate Quality of Experience (QoE) in VANETs is a critical issue in both academic and industrial communities due to dynamic network topology, importance of video QoE, and broadcast nature of VANETs. This paper presents a Qoe-Aware Reinforcement approach to disseminate warning videos on LTE-VANETs, called QAR. It enables an enhancement for routing protocols in LTE-VANETs that takes advantage of a centralized architecture around the base station to improve the route management, and to provide video dissemination with QoE support. We analyze the performance of QAR by using NS-2 simulations and a realistic urban mobility model. Results show gains of QAR in comparison to existing proposals, where it achieves video dissemination with QoE support, less routing overhead, and robustness in LTE-VANETs.*

## 1. Introduction

Nowadays, after homes and offices, vehicles are the third place where people spend the most time daily. Along with this, the possibility of integration of information and communication technologies with transportation infrastructure and vehicles over an ad-hoc network environment called Vehicular Ad-hoc NETWORK (VANET) has been broadly perceived by governments, manufacturers, and academia as a promising concept for future realization of Intelligent Transportation System (ITS) [Zaimi et al. 2016]. With videos currently accounting for more than half of the Internet traffic, new VANET applications ranging from multimedia safety and security traffic warnings to live entertainment and advertising videos have become a trend and are increasingly present [Quadros et al. 2016].

Traditional VANET consists of Vehicle-to-Vehicle (V2V) and Vehicle-to-Infrastructure (V2I) communications supported by wireless access technologies, such as IEEE 802.11p. Unlike V2V, V2I considers not only vehicles but also roadside units. However, the roadside units' deployments are very expensive, thus, modern vehicles are also envisioned to be equipped with different wireless access technologies, including interfaces to cellular communication, e.g., Long Term Evolution (LTE). In this way, a heterogeneous integration of VANETs with cellular mobile systems or connecting vehicles directly to LTE networks (LTE-VANETs) have been gaining a great attention over the past

few years. In several studies, authors have considered direct communication between cars and the LTE network [Ucar et al. 2016, Salvo et al. 2016].

Existing cellular network infrastructure, e.g., base stations (eNBs in LTE), can be employed to achieve V2I communication [Salvo et al. 2016]. However, warning video dissemination, which relies on a centralized LTE-VANET heterogeneous network must reach as many as possible vehicles going to the crash area and, at the same time, cope with other LTE traffics, e.g., Human-to-Human (H2H) and Floating Car Data (FCD) traffic. In this way, V2V communication represents a viable way to distribute significant amounts of live videos over LTE-VANETs and also alleviate congestion periods over LTE networks. In such scenario, the V2I communication takes place only for signaling and coordination of routes. As regards to the V2V communication, many challenges arise. Due to ad-hoc environment and the highly dynamic topology, connection interruptions can become frequent, very close vehicles can transmit the same packets to each other or even increasing congestion periods, etc. This all leads to an unnecessary data traffic growth, causing different impacts on the video quality and hindering action of drivers and rescue teams watching the received warning videos. Thus, dissemination of real-time video content with Quality of Experience (QoE) support is not a straightforward task.

Maximizing the user's QoE and dealing with the high vehicle mobility becomes an intricate task and has not been taken into account in most of studies to date [Quadros et al. 2016]. While QoS concentrates only on transmission statistics and network-based management, the QoE levels of the disseminated videos are associated with the subjective admeasurement of users, being key to the acceptable reception of videos [Zaimi et al. 2016]. With the presence of a centralized entity, such as LTE eNBs, it is possible to manage the broadcast routes of the videos, allowing routes to be altered as soon as data transmission problems are perceived, thus, keeping the video streaming without interruptions [Ucar et al. 2016]. In this way, the LTE-VANET routing service must be aware of QoE requirements and network conditions to recover or maintain video quality with a low overhead and high reachability in the disseminated area.

This paper presents a Qoe-Aware Reinforcement (QAR) approach to disseminate warning videos on LTE-VANETs. It enables an enhancement for routing protocols in LTE-VANETs by taking advantage of a centralized architecture around the eNB to improve route management and to provide video dissemination with QoE support. QAR uses eNBs and a traffic management server for the collection of localization and video-related parameters. Based on these data, the routing service selects the best forwarding nodes for the video dissemination. Aiming to the maintenance of routes that offer better QoE for video dissemination, QAR combines video-related parameters (e.g., different frame importance, frame position, and video distortion estimation) as well as positioning information to establish trade-offs between QoE and required hops. QAR leverages the LTE network present, admitting easily integration with different routing protocols, maintaining the packet delivery ratio, reacting positively to dynamic environments and enhancing the QoE level of the disseminated warning videos when compared to non-QoE-aware schemes. We add QAR to a straightforward distance-based protocol and evaluate its performance. Results show gains of QAR in comparison to existing proposals, where it achieves video dissemination with QoE support, less routing overhead, and robustness in LTE-VANETs.

We organize this paper as follows. Section 2 outlines the related work. Section 3 introduces the QAR approach. Section 4 shows simulation setup and results comparing current LTE-VANET-based works and QAR. Lastly, Section 5 presents the conclusions.

## 2. Related Work

Recently, many authors have proposed routing protocols for LTE-VANETs. LTE provides data dissemination to many users over a geographical area at fine granularity. Most of current schemes assume that vehicles transmit application data directly to eNBs or through clustering schemes (i.e., cluster members communicate with cluster heads by using IEEE 802.11p and cluster heads communicate with eNBs by using LTE). [Ucar et al. 2016] presented a hybrid architecture, namely VMaSC-LTE, which combines IEEE 802.11p clustering and LTE with the goal of achieving high packet delivery rate with a minimum usage of the LTE infrastructure. [Salvo et al. 2016] proposed a FCD off-loading scheme via clustering formation in a LTE-VANET. [Jia et al. 2014] introduced a Markovian-based model to mitigate FCD transmissions. These works aim to reduce the traffic rates transmitted over the LTE, however, they do not examine transmissions of long data traffic, e.g., real-time warning videos, and do not consider video-related parameters for decision-making. Besides, a pure LTE based architecture is not feasible for vehicular communication due to the overload of the eNBs by packets coming from a high vehicle traffic density, which directly impacts other LTE flows, e.g., FCD and H2H [Salvo et al. 2016].

In this way, hybrid architectures represent a viable way to transmit warning videos over LTE-VANETs, and to alleviate congestion over LTE networks. The V2I communication proceeds only for signalling and route management and discovery, while V2V communication proceeds for the video distribution. There are three strategies for data dissemination used to design many routing protocols, including hybrid schemes with topological approaches: distance-, location-, and counter-based [Gonzalez and Ramos 2016]. In these strategies, nodes decide by themselves if they further broadcast data or not through a distributed backoff phase (i.e., by comparing a locally measured value). In distance-based protocols, forwarding node candidates use only the distance to the farthest 1-hop neighbor from whom the packets has been sent as a proxy for rebroadcasting [Chang and Lee 2015, Slavik et al. 2015]. In location-based protocols, nodes share location information to allow retransmissions in the uncovered areas [Mir et al. 2016, Husain and Sharma 2016]. Lastly, in the counter-based protocols, nodes count the number of times that each packet is received during the backoff time to know the number of neighbors that so far have retransmitted the packets [Chekhar et al. 2016, Torres et al. 2015].

[Slavik et al. 2015] presented a Distance-to-Mean (DTM) method, which extends the distance-based strategy, where nodes rebroadcast packets as soon as they cover a large amount of physical area that neighboring nodes have not covered. Likewise, [Torres et al. 2015] introduced an Automatic Copies Distance-Based (ACDB) mechanism, which extends the Counter-based strategy to cope with variable vehicle density situations. Despite ACDB applies Peak Signal-to-Noise Ratio (PSNR) to assess the QoE of received videos, the main drawback of the above approaches consists of their reliance on a single positioning parameter to compute the backoff phase. This issue reduces the network reliability for long data transmission, e.g., live videos. Further, PSNR evaluation does not correlate well with the subjective acceptability of the users [Quadros et al. 2016]. Using a decentralized organization is totally justified in these works, since authors assume

that vehicles have a single IEEE 802.11p interface, and no cellular network interface. However, the latest technological advances enable vehicles to be equipped with multiple types of wireless interfaces, forming a multihomed heterogeneous network environment.

From our analysis, there are several approaches for video dissemination in LTE-VANETs. For V2V communication, approaches where nodes decide by themselves if they must retransmit data or not, are promising, since vehicles do not flood messages proactively, avoiding routing overhead. With vehicles equipped with LTE interfaces, it is possible to improve the management of flow dissemination. Further, existing proposals do not apply video-related parameters to reinforce the video dissemination, neither offer this key feature in a unified routing protocol so far, lacking of robustness and QoE-awareness.

### 3. The QoE-Aware Reinforcement (QAR) Approach

This section presents the QAR approach to reinforce the dissemination of warning videos in LTE-VANETs. It relies on a centralized structure around the VANET area, avoiding neighboring information exchange. QAR works jointly with an underlying routing protocol and intends to select forwarding nodes with high reachability, i.e., nodes that deliver videos to as many destinations in a physical area as possible. This refrains unnecessary routing overhead and impact on the existing LTE traffic, i.e., FCD and H2H. Further, QAR allows video dissemination with QoE support even in face of dynamic topology scenario changes. QAR runs on the infrastructure to establish QoE-aware routes for video dissemination, where it considers vehicles' location and video-related parameters for forwarding decision. Depending on the routing protocol, QAR can combine other different parameters, aiming at a more in-depth decision process, e.g., link quality, speed, etc.

QAR works in two phases, namely Contention-Based Forwarding (CBF), and Centralized QoE-supported Management (CQM) phases. In the CBF phase, the Source Node (*SN*) indicates through its LTE network interface that it will begin a video broadcast and it starts the video flooding. Thereon, the Forwarding Node Candidates (*FNCs*) compete with each other to participate in the transmission routes (i.e., Forwarding Nodes - *FNs*). The *FNCs* take into account positioning and video-related parameters for forwarding decision, where the winning nodes retransmit the video sequences further. The CQM phase considers V2V forwarding and V2I management, exploiting the previously built multi-hop paths in CBF, and enabling dynamic changes to other *FNs* in case of link failures or low QoE detection. We will detail each phase in the following subsections.

In our network model, let us suppose a scenario of warning video dissemination in cases of accidents or disasters, where vehicles or first responder teams, coming toward the crashed area, receive in advance the real-time videos of the accident from a *SN*. We consider  $k$  vehicles with identifiers ( $i \in [1, k]$ ), moving over an multi-lane highway area. The combination of those nodes configures a graph  $G(V, E)$ , where vertices  $V = \{v_1, v_2, \dots, v_k\}$  mean a finite subset of  $k$  nodes, and edges  $E = \{e_1, e_2, \dots, e_m\}$  mean a finite set of asymmetric wireless links between them. We denote  $N(v_i) \subset V$  as a subset of all 1-hop neighbors within the radio range of a given node  $v_i$ . Further, each node  $v_i$  has an IEEE 802.11p-compliant radio transceiver, through which it can communicate with  $N(v_i)$ , a LTE interface that allows each node  $v_i$  to be managed directly by a traffic server (nodes can also be managed by eNBs when it is possible to implement that directly in the eNB). Moreover, each  $v_i$  holds a GPS (to location awareness and synchronism in time),

a multimedia encoder/decoder, and a transmission buffer. Fig. 1 shows a simplified node architecture with QAR (Subsection 3.1), IEEE 802.11p and 3GPP LTE radios, and other interdependent elements of a node. Table 1 outlines the main symbols used in this paper.

**Table 1. The main symbols used in the QAR description.**

Symbol	Description
$v_i$	A node with an Id ( $i \in [1, k]$ )
$N(v_i)$	Set of 1-hop neighbors of $v_i$
$SN$	Source Node
$FNC$	Forwarding Node Candidate
$FN$	Forwarding Node
$MS$	Management Server
$VF$	Video Flow
$W(VF)$	Time Window to broadcast pkts
$WZ$	Warning Zone
$FF$	Fit Function
$Pos_{param}$	Positioning parameter of $FF$
$Vid_{param}$	Video-related parameter of $FF$

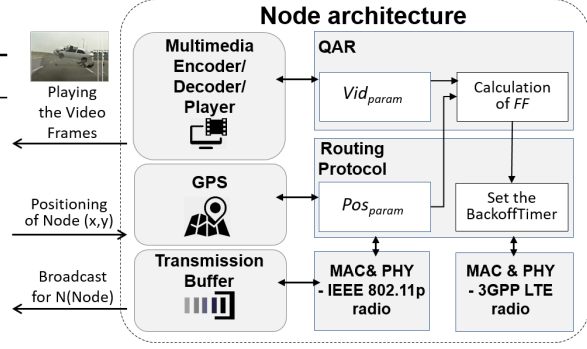


**Figure 1. Simplified node architecture with QAR.**

### 3.1. Contention-Based Forwarding (CBF)

At the beginning of the CBF phase of QAR,  $SN$  warns eNB that it will start a video dissemination through its LTE network interface. Particularly,  $SN$  sends a Notification to Video Broadcast (NVB) to a Management Server ( $MS$ ), which assumes that  $SN$  is the initial node. The NVB contains the current  $SN$  position and a video Id  $\langle SN_{pos}, SN_{Id} \rangle$ . Vehicles periodically send FCD to the  $MS$  in LTE, which contains information about presence, position, kinematics, or basic status [Jia et al. 2014]. The  $MS$  selects the  $FNCs$  that will compete to retransmit the video packets, based on  $SN$  positioning parameters and neighbors previously collected by FCD. Alg. 1 presents the CBF process performed at the  $MS$ . Firstly,  $MS$  obtains, from its FCD table, the current and past position of the broadcasting node ( $v_a$ ) and its neighbor nodes  $N(v_a)$  (Lines 1, 2, 4, and 5 of Alg. 1). In addition,  $MS$  establishes a Warning Zone ( $WZ$ ) to limit the dissemination area, i.e., for a video exceeding a predetermined  $WZ$ , no further rebroadcast occurs (Line 3 of Alg. 1). We defined  $WZ = 2km$ , based on radio range of 250m in each hop and considering 8 as the maximum number hops for each path. This  $WZ$  provides a medium-long distance, as required in many rescue/disaster VANET scenarios [De Felice et al. 2015].

To limit the video dissemination for only vehicles going to the crash area,  $MS$  compares the angle between current and past position of  $v_a$  and current position of each  $v_k \in N(v_a)$  to a threshold angle  $\phi = 90^\circ$  (Line 7 and 8 of Alg. 1). If the angle is greater than  $\phi$ ,  $MS$  performs a new comparison. The conditions mentioned above allow the system to mitigate the number of  $FNCs$  and the overhead of video packets by selecting only vehicles interested in the video. Thus, vehicles that have already passed by the accident area and vehicles going in the opposite direction will not need to receive the videos. The angle  $\phi$  can be modified depending on the scenario, roads, or reachability rates of the routing service. As soon as the  $MS$  calculates the chosen  $FNCs$ , it sends an Authorization to Video broadcast (AVB) to  $FNCs$  and  $SN$ . In this way, the  $SN$  starts the broadcast of a Video Flow  $VF$  to its neighbors vehicles in a multi-hop fashion, i.e.,  $SN$  broadcasts video packets  $p$  in a Time Window, denoted by  $W(VF_i) \subset VF_i$ , to all its neighbors ( $N(SN)$ ). All nodes that were not chosen by  $MS$  to become  $FNCs$ , drop

$W(VF_i)$  at the MAC layer and, therefore, do not increasing network overhead. Through a contention distributed stage  $FNC$ s compete among themselves to choose which nodes will become Forwarding Nodes ( $FN$ s). Alg. 2 presents the process of CBF at the  $FNC$ s.

---

**Algorithm 1** CBF phase in the Management Server ( $MS$ )

---

When a given node  $v_a$  (with  $|N(v_a)|$  1-hop neighbors) sends a  $NVB_i$

$k \leftarrow 0$

- 1: Retrieves  $v_a(x_{t-1}, y_{t-1}), v_a(x_t, y_t)$
- 2: **if**  $v_a SN < WZ$  **then** //Detecting if  $WZ$  is established
- 3:     **while**  $k < |N(v_a)|$  **do**  $\forall v_k \in N(v_a)$
- 4:         Retrieves  $v_k(x_{t-1}, y_{t-1}), v_k(x_t, y_t)$
- 5:         **if**  $\angle v_a(x_t, y_t)v_a(x_{t-1}, y_{t-1})v_k(x_t, y_t) > \phi$  **then**
- 6:             **if**  $\angle v_a(x_t, y_t)v_a(x_{t-1}, y_{t-1})v_k(x_{t-1}, y_{t-1}) \geq \angle v_a(x_t, y_t)v_a(x_{t-1}, y_{t-1})v_k(x_t, y_t)$  **then**
- 7:                  $v_k \leftarrow FNC$
- 8:                 Sends  $AVB_i$  to  $v_k$
- 9:             **end if**
- 10:         **end if**
- 11:          $k++$
- 12:     **end while**
- 13:     Sends  $AVB_i$  to  $v_a$
- 14: **end if**

---



---

**Algorithm 2** CBF phase in Forwarding Node Candidates ( $FNC$ s)

---

When a given node  $v_b \in N(v_a)$  receives broadcasted packets ( $W(VF_i) = \sum_{k=1}^n p_k$ ) from a node  $v_a$ :

- 1: **if**  $v_b \supset AVB_i$  **then** // Detecting if  $v_b$  is a  $FNC$ .
- 2:     **if**  $\exists! p_k \in W(VF_i)$  **and**  $v_b \supset p_k$  **then** // Detecting redundant packets.
- 3:         Drop  $W(VF_i)$  from  $v_b$
- 4:         **return**
- 5:     **else**
- 6:         Sends  $NVB_i$  to  $MS$
- 7:         Compute  $FF(v_b)$  (Eq. (6))
- 8:         Start  $BackoffTimer(v_b)$  (Eq. (1))
- 9:         **while**  $BackoffTimer(v_b) \neq 0$  **do**
- 10:             **if** Overhear  $! p_k \in W(VF_i)$  **then** // Detecting redundant packets.
- 11:                 **if**  $\angle FNv_av_b < \lambda$  **then** // Angle comparison between  $FN$  and  $v_b$ .
- 12:                     Cancel  $BackoffTimer(v_b)$
- 13:                     Drop  $W(VF_i)$  from  $v_b$  **and** Cancel any new rebroadcast of  $p_k \in W(VF_i)$
- 14:             **return**
- 15:             **end if**
- 16:         **end if**
- 17:         **end while**
- 18:         Rebroadcasts  $W(VF_i)$  **and**  $v_b \leftarrow FN$
- 19:     **end if**
- 20: **end if**

---

If  $v_b$  has already received an  $AVB_i$  from  $MS$  to forward the video packets and if  $W(VF_i)$  contains only new received packets (Line 2 of Alg. 2),  $v_b$  sends a  $NVB_i$  to  $MS$  and apply the *Fit Function* ( $FF$ ) (Eq. (6)) (Line 7 of Alg. 2).  $FF$  allows the network to mitigate the number of retransmissions and duplicated packets by choosing only the best  $FNC$ s. The value of  $FF$   $[0, FF_{max}]$  depends on parameters of the underlying routing protocol, such as positioning (Subsection 3.1.2), and video-related parameters, as shown in Subsubsection 3.1.1. Thus, after calculating the  $FF$ ,  $v_b$  sets a  $BackoffTimer$  according

to Eq. (1), and after the timeout, rebroadcasts the buffered packets ( $W(VF_i)$ ). It is easy to see that nodes with higher values of  $FF$  are mapped to smaller  $BackoffTimer$  values, and thus have a higher probability to forward the video packets.

$$BackoffTimer = CW_{Max} - FF \cdot (CW_{Max} - CW_{Min}) \quad (1)$$

Where  $CW$  [ $CW_{Min}, CW_{Max}$ ] is the size of the *Contention Window* in the 802.11p standard. The  $FNC$  that generates the smallest  $BackoffTimer$  rebroadcasts  $W(VF_i)$  first and becomes a  $FN$  (Line 18 of Alg. 2). Moreover, as expected in the IEEE 802.11p standard, vehicles are able to sense the channel during the  $BackoffTimer$ . Thus, in case of overhearing transmissions from another  $FN$ ,  $v_b \in N(FN)$  compares the angle between its own location,  $FN$ , and the sender node ( $v_a$ ) to a threshold angle  $\lambda = 45^\circ$ . This threshold angle implies directly the reachability of the routing protocol (Line 11 of Alg. 2). When the angle between the previous selected  $FN$  and  $v_b$  is bigger than  $\lambda$ ,  $v_b$  proceeds to retransmit  $W(VF_i)$  itself, otherwise it remains silent. With this strategy, the received packets can be disseminated to other directions via multiple  $FN$ s.

In the next subsections, we will describe how QAR uses both, video-related and positioning parameters to compute  $FF$  and, thus, to choose the best  $FN$ s. The selected  $FN$ s retransmit the video flows to neighbors until  $WZ$  be reached and participate in the CQM phase, where dynamic routes of dissemination are built (Subsection 3.2).

### 3.1.1. Video-related parameters

Each packet  $p$  in a  $VF$  contains, in addition to the data payload, other encoder parameters, such as a frame-type flag, Id, length, timestamp, and packet segmentation. To obtain this information, the Deep Packet Inspection (DPI) algorithm enables extraction of the frame type and intra-frame dependency information for each  $p$  [Sherry et al. 2015], since each  $VF$  starts with a Group of Pictures (GoP) header and by one or more coded frames. The DPI methods have been used in existing works to collect information about malicious packets, frame type and intra-frame dependency, which are described in the video sequence and GoP headers [Quadros et al. 2016]. Thus, DPI is a good alternative to allow cross-layer multimedia networking solutions to improve the usage of network resources and the user's perception.

Regarding to the video structure, MPEG-4 video sequences are compressed in GoPs composed of I (Intra), P (Predictive), and B (Bidirectional) frames. Frames between two I-frames belong to one GoP, so that there is no fixed value for the GoP size (generally, 10-20 frames). I-frames are self-contained, however, to encode and decode P- and B-frames, the previous I-frame and/or P-frames in the same GoP are needed. Thus, when an I or P-frame is lost, all frames thereafter in the GoP become un-decodable, i.e., the same degree of packet loss may cause severe video quality degradation or may pass unnoticed, depending on which frame types are affected. Fig. 2 shows the different importance degrees for the user's perception in each frame type for an 18-frames GoP size. The length of a loss burst determines the number of subsequent frames in which this effect propagates. I-frames are the most important ones, followed by P-frames and, finally, B-frames (for a single B-frame lost, no impact is noticed visually, since no other frames are affected). Further, the loss of P-frames at the beginning of a GoP causes a higher video

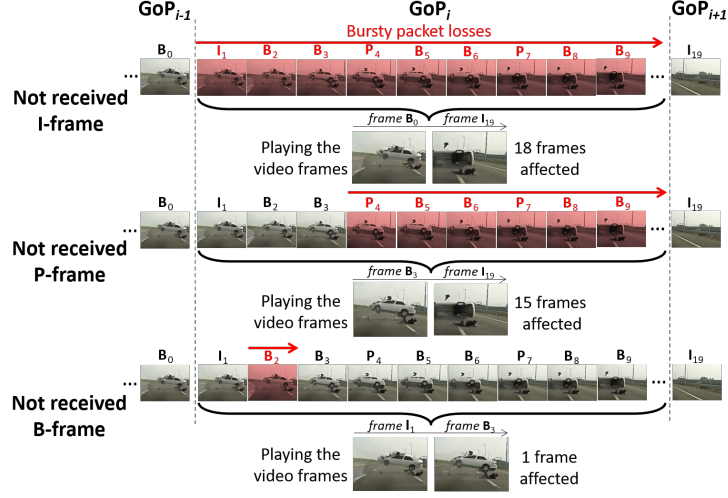


**Figure 2. Different priority of frames.**

distortion as detailed in [da Silva et al. 2016]. By considering the importance of each video frame, as well as the P-frame position within a GoP, QAR prioritizes frames with a greater impact on the average video distortion ( $\sigma_s^2$ ). Thus, it assigns different weights to packets belonging to each frame as modeled by Eq. (2):

$$\sigma_s^2 \propto \begin{cases} \frac{\alpha_1(R_M - R_I)}{R_M} & \text{if } s \in \text{I-frame} \\ \frac{\alpha_2}{(2^{T-1}-1)R_M} \sum_{i=1}^{T-1} 2^{T-1-i}(R_M - R_{P_i}) & \text{if } s \in \text{P-frame} \\ \frac{\alpha_3(R_M - R_B)}{R_M} & \text{if } s \in \text{B-frame} \end{cases} \quad (2)$$

Where  $T-1$  is the total of P-frames per GoP,  $R_I$ ,  $R_{P_i}$ , and  $R_B$  mean the I, P (with position  $i$  in the GoP), and B-frame received rate in  $W(VF_i)$ , respectively.  $R_M$  is the maximum data-rate supported by the radio transceiver of each vehicle, e.g., for a DCMA-86P2 IEEE 802.11p Wi-Fi card,  $R_M = 6\text{Mbps}$  if  $P_{rx} > -93\text{dbm}$  [Quadros et al. 2016]. The parameters  $\alpha_1$ ,  $\alpha_2$ , and  $\alpha_3$  are weighting factors, where  $\sum_{i=1}^3 \alpha_i = 1$ .

The distortion model proposed by Shu Tao [Tao et al. 2008] considers the impact caused by the loss of packets of a video frame. Thus, for a video frame structure and a probability of occurrence of loss, Eq. (3) defines an overall distortion value for the whole stream, where  $L$  is the number of packets per frame obtained from the MPEG-4 configuration and packetization. The parameter  $\bar{n}$  represents the loss burstiness ( $1.06 \geq \bar{n} \geq 1$  for Bernoulli losses, depending on the aggressiveness of the burst errors). The attenuation factor  $\gamma$  ( $\gamma < 1$ ) accounts for the effect of spatial filtering, and varies as a function of the video characteristics and decoder processing.  $P_e$  is the probability of loss events (of any length) in the video stream. Both,  $\gamma$  and  $P_e$  are given by the effect of the loss pattern experienced by the video stream and the codec's error concealment technique. Finally, the Mean Square Error (MSE) distortion  $\bar{D}$  provides a QoE-estimate ( $Vid_{param}$ ) by using a non-linear relation that measures the video quality level by comparing distortions caused by packet losses [Tao et al. 2008], according to each frame type, denoted in Eq. (4):

$$\bar{D} = L \cdot \bar{n} P_e \cdot \sigma_s^2 \cdot \left( \frac{\gamma^{-T+1} - (T+1)\gamma + T}{T(1-\gamma)^2} \right) \quad (3)$$

$$Vid_{param}^{v_b}(W(VF_i)) = \frac{1}{1 + \exp(b_1 \cdot 10 \cdot \log_{10}(255^2/\bar{D}) - b_2)} \quad (4)$$

Where,  $b_1$  is the slope of the QoE mapping curve and  $b_2$  is the central point. By considering 40 dB as the highest video quality, and the lowest video quality for values below 20 dB, the values of  $b_1$  and  $b_2$  are given by 0.5 and 30, respectively. Based on the average distortion caused by losses in the different frame types in  $W(VF_i)$  it is possible for  $FNCs$  to compute a higher  $FF$  based on receiving the most important packets.

### 3.1.2. Coupling of the CBF phase of QAR with the Distance-Based Routing Protocol

This subsection presents QAR operating together with an underlying routing protocol. To assess QAR functionalities, we develop and adapt its CBF stage jointly with a straightforward broadcast protocol built using the distance-Based strategy, called DQAR protocol. Distance-based protocols calculate coverage through the distance ( $Pos_{param}$ ) from the  $FNC$  to the previous sender node. When  $Pos_{param}$  is small, it means the  $FNC$  is close to the last sender, indicating it should not favor rebroadcasting. Only local positioning information is used in the distance-based strategy to calculate  $Pos_{param}$  in  $FNCs$ . Thus, the spatial distance is defined according to Eq. (5) for a  $FNC$  positioned at  $(x, y)$  and a previous sender node located at  $(\bar{x}, \bar{y})$  and normalized to a value between zero and one by dividing by the maximum transmitting range ( $R$ ) of the vehicles. Hence,  $FNCs$  with large geographical distance from previous sender node generate higher  $FF$  values.

$$Pos_{param} = \frac{1}{R} \sqrt{(x - \bar{x})^2 + (y - \bar{y})^2} \quad (5)$$

To add QAR with the distance-based protocol, we establish two parameters as input to  $FF$  (Eq. (6)): vehicle positioning ( $Pos_{param}$ ) and video-related parameters ( $Vid_{param}$ ), allowing a cross-layer selection of  $FNCs$  (Fig. 1) in addition to the only positioning parameters of the pure distance-based protocol. As defined in Eq. (5), the distance-based protocol does not exchange messages containing location or mobility information. Thus, DQAR also mitigates the overhead when determining the best  $FNC$  options ( $FNs$ ). Further, the QAR steps can be easily adapted to other routing protocols by simply changing the parameters in the CBF stage for the  $FN$  selection process. It might be suitable for link quality-based, stochastic-based, or counter-based routing protocols.

### 3.2. Centralized QoE-supported Management (CQM)

As video transmissions have often long duration (e.g., 20 s), whenever a  $FNC$  wins the CBF phase,  $SN$  transmits video packets explicitly without any additional delay and in a pipeline fashion along the built route. Thereby, QAR reduces additional delays and packet duplication from the CBF phase by introducing the Centralized QoE-supported Management (CQM) phase. During the transmission, nodes must deliver the video content even in the presence of link failures or channel variations. QAR detects routing failures, providing a smoother route management by considering that every  $FN$  that composes the video dissemination routes should perceive whether it is still a reliable or valid route to transmit packets. This is achieved by receiving reply messages. We define a control packet, called Quality Warning Message (QWM), which contains the  $\bar{D}$  perceived by each  $FN$ . Thus, if a  $FN$  receives a video flow, it must compute  $\bar{D}$  (distortion) perceived in each  $W(VF)$  and send a QWM to  $MS$ . A route in CQM returns to the CBF phase, when  $MS$  is notified that the video quality fallen below a predefined video distortion threshold. Further,  $MS$

considers that the route is not valid anymore, as long as it does not receive any QWM from  $FN$ s within a certain period of time, i.e.,  $\text{timeout} = 0.5s$ . Hence, it sends an AVB to the previous  $FN$  and the route returns to the CBF phase.

Upon computing  $Vid_{param}$  and  $Pos_{param}$ , each  $FN$  contains the two calculated parameters of the  $FF$ , i.e.,  $P = \{Vid_{param}, Pos_{param}\}$  ( $|P| = 2$ ). Thus, considering the different weights  $\omega_j$   $\sum_{j=1}^{|param|} \omega_j = 1$ , Eq. (6) calculates  $FF$  by multiplying the values  $p_j$  in  $P$  and the weights of the evaluation parameters, similarly to others multi-criteria approaches [Jauregui and Malaina 2016]. From Eq. (6), other parameters can be added to  $FF$  of QAR, depending only on the underline routing protocol.

$$FF = \sum_{j=1}^{|P|} (p_j \times \omega_j) \quad (6)$$

#### 4. Performance Evaluation

This section shows methodologies and metrics used to evaluate the transmitted video flows, and we compare the performance of DQAR with the main related works. To a proper scenario, we have considered a 10 Km portion of the San Diego Freeway, imported into Simulation of Urban MObility (SUMO), to reproduce the vehicle movements and interactions according to empirical data. In our simulations, vehicles move ranging from 20 to 30 m/s, each one holding an IEEE 802.11p (5.89 GHz, 6 Mbps) radio with about 250 m transmission range and a 3GPP LTE (700 MHz, 300 Mbps) radio with a transmission range up to 30km. We applied the Nakagami Fading Channel as propagation model. Similarly to [Torres et al. 2015], we scheduled an accident situation, so that when  $SN$  perceives this accident, it sends a  $NVB$  to  $MS$  and starts the broadcast of  $VF$ . Each  $VF$  must be received by vehicles within a  $WZ = 2\text{km}$  from  $SN$ , providing limitation of hops. The Radio Access Network (RAN) consists of eNBs, which manage radio resources and handover events. ENBs connect a Serving Gateway/PDN Gateway (SGW/PGW) via Evolved Packet Core (EPC) network, that contains a Mobility Management Entity (MME) with the  $MS$ , responsible for store vehicles' position information.

For the purpose of realistic results, we have adopted the EvalVid framework- A Video Quality Evaluation Tool-set that allows us evaluating the video quality. Thus, we have conducted the experiments by transmitting real MPEG-4 sequences (720 x 480 pixels) lasting approximately 20 s, available in [Video Sequences 2016a], with 768 kbps and 24 fps, internal GoP structure (size 20) configured as two B-frames for each P-frame. Finally, we added the videos and the road/vehicle features into Network Simulator 2.33.

To demonstrate the impact of DQAR (QAR coupled with a distance-based protocol), we used DTM [Slavik et al. 2015], ACDB [Torres et al. 2015], and a straightforward routing protocol built from the distance-based strategy (named DIST) for comparison. The DTM and ACDB protocols use distance-based and counter-based strategies, respectively. In DTM, the farther away the node to the spatial mean, the shorter the *BackoffTimer*. ACDB uses vehicles' density information to dynamically adjust a counter and the maximum  $FF$  before rebroadcasting packets. We adjusted these protocols with the CQM phase to reduce the contention phase: once a vehicle successfully transmits video packets, its timer for the next packets will be minimum. Further, we added each protocol to nodes with IEEE802.11p and LTE interfaces, where the eNB performs the

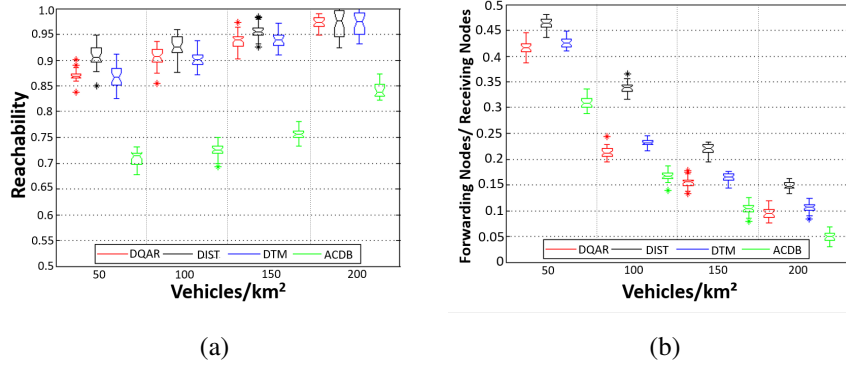


**Figure 3. Reachability and Forwarding Nodes by Receiving Nodes vs Veh/km<sup>2</sup>**

selection of  $FNC$ s for each protocol. We introduced these improvements because the standard protocols, as they were, did not represent a fair comparison.

The I-, P-, and B-frame weights ( $\alpha_1$ ,  $\alpha_2$ , and  $\alpha_3$ ) influence the QAR performance. We have conducted independent empirical evaluations and we concluded that  $\alpha_1 = 0.65$ ,  $\alpha_2 = 0.3$ , and  $\alpha_3 = 0.05$  give the best  $Vid_{param}$  results. Moreover, the weights for each parameter  $\omega_1$  and  $\omega_2$  were fixed in 0.6 and 0.4, respectively, which allow QAR to achieve the best trade-off between the lowest number of hops and the enough QoE-indicators to assure the video delivery with an acceptable video quality level. In addition, we set  $CW_{Max}$  to 100ms,  $W(VF)$  to 80ms, and  $\bar{D}_t$  to 0.75.

We assessed the above protocols by reachability, i.e., the average fraction of nodes that receive the broadcasted videos, number of  $FN$ s over receiving nodes, Packet Delivery Rate (PDR), and average delay. Since measuring the human experience is key for our work, we carried out QoE-based measurements with a well-known objective QoE metric, called Structural SIMilarity (SSIM) [Quadros et al. 2016]. SSIM measures the structural distortion of the video to obtain a better correlation with the user's perspective. We obtained results by varying number of vehicles (50 - 200 veh/km<sup>2</sup>) and distance to the crash area (500 - 2000m), being an average of 35 simulations (95% confidence level). Each simulation lasts 500s, where, a  $SN$  sends a  $VF$  at any time after the initial 100s and before the last 100s.

Fig. 3a shows DQAR, DIST, and DTM outperforming ACDB in terms of reachability, due to the latter unconsider positioning parameters to selection of  $FN$ s (counter-based protocol). When in 50 Veh/km<sup>2</sup>, all protocols achieve a less reachability due to irregular mobility and distribution of vehicles in the network, causing void areas. When between 150 and 200 Veh/km<sup>2</sup>, all the distance-based protocols perform with reachability between 93% and 99%, since for high density scenarios, the route options are greater, leading to fewer broken links and a bigger coverage of protocols. On average, DQAR and DTM increase reachability by 15.3% and 14.8% compared to ACDB, respectively, while DIST increases reachability by 4.2% and 5.3% over DQAR and DTM, respectively. The highest reachability of DIST occurs due to the selection parameters of DQAR and DTM, where  $FN$ s are close nodes that experience more stable connectivity.

Fig. 3b shows the number of  $FN$ s over receiving nodes as a measure of the protocols efficiency. The smaller the number of  $FN$ s with satisfactory reachability for a video broadcast, the more efficient is the protocol. In Fig. 3b, DQAR and DTM have similar

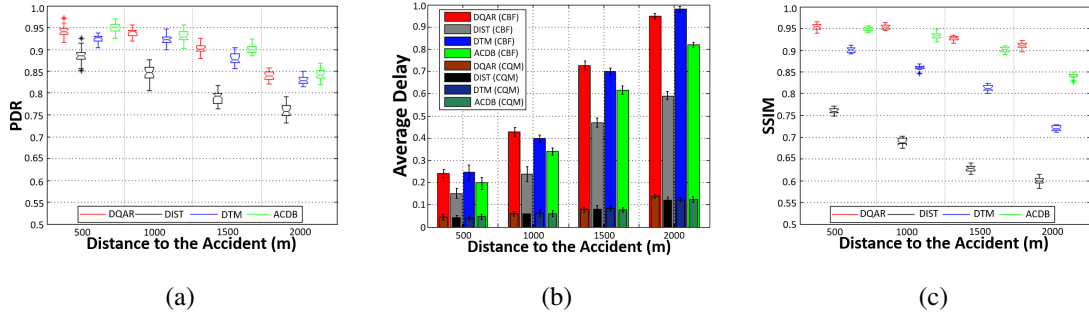


**Figure 4. PDR, Average Delay, and SSIM vs Distance to the Accident**

behavior, however, DIST provides a lower performance, whereas ACDB achieves good results when compared to DQAR and DTM. DQAR, DIST and DTM are identical except DIST uses only the distance-based strategy, DTM uses the Distance-to-Mean strategy, and DQAR uses distance-based strategy coupled with video-related parameters to reinforce the QoE. ACDB has an adaptive  $FF$ , which depends on the density of vehicles. Thus, the more vehicles, the lower the  $FF$  for transmission, leading to a smaller number of  $FN$ s per receiving nodes. In Fig. 3a, DQAR, DTM, and DIST exhibit a close reachability. However, in terms of number of  $FN$ s to accomplish that level of reachability, DQAR and DTM uniformly consume less bandwidth than DIST. Finally, despite these apparent good findings in terms of overhead and efficiency, ACDB does not achieves a good reachability, thus, it does not performs satisfactorily for warning video dissemination over VANETs.

Regarding the performance in terms of PDR and average delay, Figs. 4a and 4b show the performance results for the four simulated protocols for vehicles located within different distances from the accident region when the transmission of video packets was initiated. As aforementioned, DIST achieves a high reachability, but faces several broken link situations leading to a low PDR. Otherwise, ACDB reaches a PDR slightly higher in comparison to DTM, i.e., around 3.1%. This is because sometimes DTM elects farthest relay nodes such as DIST, mainly when there are few neighboring vehicles. Otherwise, ACDB adapts its  $FF$  depending on the number of neighbors, thus, increasing PDR.

The impact of the CBF and CQM phases are meaningful on the delivery delay over the transmissions (Fig. 4b), since CQM allows a great reduction of the average delay by using a contention-free forwarding. Here, we consider the average delay required by a  $W(VF)$  to be transmitted in a range starting from  $SN$ . DIST at CBF stage experiences the lower delay, due to the reduced number of hops achieved by the distance-Based strategy. After, DIST is followed by ACDB, because this protocol reduces its *BackoffTimer* when in presence of few nodes. In addition, when DIST is compared with DQAR and DTM, the delay reduction provided by DIST is significant, e.g., around 40.2% and 38.6%, respectively for 1000m of range. As aforementioned, DQAR, unlike DIST and according to its forwarding parameters, provides more effort to transmit flows with high QoE, this could mean forwarding streams to closer nodes, increasing the average delay. However, the achieved delay levels are negligible even in video applications and are significantly lower than the requirements of 4 to 5 s defined by CISCO [Index 2013].

As discussed before, QoS-based metrics (e.g., PDR) are not enough to measure the quality level from the user's perspective. Thus, aiming to understand and confirm

the impact of the video-related parameters, the results in Fig. 4c present the SSIM metric. SSIM values range from 0 to 1, where higher values mean better video quality. In Fig. 4c, DQAR keeps the SSIM values about 0.97 and 0.9. An average increase of 27.2%, 18.1%, and 8.3% compared to DIST, DTM, and ACDB, respectively. It presents more deeply results than those obtained in Fig. 4a and shows significant benefits to the user's experience. This occurred because DQAR perceives when the QoE of the transmitting flow decreases based on the different received frame types, codec configurations, and losses, allowing eNB and vehicles, through  $FF$  calculation, to switch to others nodes, before increasing damage on the flow quality. For instance, let us suppose a  $W(VF_i)$  successfully received by a  $VR_i$  in  $|W(VF_i)|$  ms. As the spatial distribution of vehicles does not change very quickly in a short period of time (e.g., 3 s), it is likely that  $VR_i$ , continue to receive successfully a greater number of packets until a new route becomes necessary. Thus, DQAR provides a trade-off between hop-length and video quality. Aiming to give the reader an idea of the user's point-of-view, in [Video Sequences 2016b], we provide some simulated video samples for comparison between the four evaluated routing protocols in this paper.

## 5. Conclusion

In this paper, we introduced QAR to optimize warning video dissemination with QoE-awareness in LTE-VANETs. QAR aims to share videos with a better quality than existing works by applying video-related parameters to the selection of forwarding nodes and changing routes as soon as the video quality levels are below to a QoE-aware threshold. Results highlighted the performance and QoE-awareness of QAR by measuring the video quality levels when the distance to the sender varies. From our analysis, we identified that the distance-based protocols (i.e., DIST and DTM) perform poorly compared to DQAR in terms of QoE assurance. Despite this, these protocols have obtained similar delivery rate and average delay levels. According to its forwarding parameters, QAR provides a greater support to dissemination of video flows with higher quality from the user's point-of-view. This could mean forwarding of streams to alternative nodes by increasing transmission delays, but nonetheless, still are insignificant to the real-time video requirements. In future works, we will perform a study with other video features (e.g., GoP size and packetization), so that  $FF_t$  can be dynamically adjusted to better performance.

## References

- Chang, S.-w. and Lee, S.-s. (2015). Distance-based stable routing decision scheme in urban vehicular ad hoc networks. *Int. Journal of Distributed Sensor Networks*, 2015:3.
- Chekhar, M., Zine, K., Bakhouya, M., and El Ouadghiri, D. (2016). An efficient broadcasting scheme in mobile ad-hoc networks. *Procedia Computer Science*, 98:117–124.
- da Silva, C., Ribeiro, E., and Pedroso, C. (2016). Preventing quality degradation of video streaming using selective redundancy. *Computer Communications*, 91:120–132.
- De Felice, M., Cerqueira, E., Melo, A., Gerla, M., Cuomo, F., and Baiocchi, A. (2015). A distributed beaconless routing protocol for real-time video dissemination in multimedia vanets. *Computer Communications*, 58:40–52.
- Gonzalez, S. and Ramos, V. (2016). Preset delay broadcast: a protocol for fast information dissemination in vehicular ad hoc networks (vanets). *EURASIP Journal on Wireless Communications and Networking*, 2016(1):1–13.

- Husain, A. and Sharma, S. (2016). Performance analysis of location and distance based routing protocols in vanet with ieee802. 11p. In *3rd International Conference on Advanced Computing, Networking and Informatics*, pages 215–221. Springer.
- Index, C. V. N. (2013). Global mobile data traffic forecast update, 2012–2017, cisco white paper, feb. 6, 2013.
- Jauregui, B. B. and Malaina, F. L. (2016). new approaches to mobile ad hoc network routing: Application of intelligent optimization techniques to multicriteria routing. *Mobile Ad Hoc Networks: Current Status and Future Trends*, page 171.
- Jia, S., Hao, S., Gu, X., and Zhang, L. (2014). Analyzing and relieving the impact of fcd traffic in lte-vanet heterogeneous network. In *Telecommunications (ICT), 2014 21st International Conference on*, pages 88–92. IEEE.
- Mir, Z. H., Kim, J., Ko, Y.-B., and Filali, F. (2016). Improved multi-hop routing in integrated vanet-lte hybrid vehicular networks. In *10th International Conference on Ubiquitous Information Management and Communication*, page 76. ACM.
- Quadros, C., Santos, A., Gerla, M., and Cerqueira, E. (2016). Qoe-driven dissemination of real-time videos over vehicular networks. *Computer Communications*, 91:133–147.
- Salvo, P., Turcanu, I., Cuomo, F., and Baiocchi, A. (2016). Lte floating car data application off-loading via vanet driven clustering formation. In *12th Annual Conference on Wireless On-demand Network Systems and Services (WONS)*, pages 1–8. IEEE.
- Sherry, J., Lan, C., Popa, R. A., and Ratnasamy, S. (2015). Blindbox: Deep packet inspection over encrypted traffic. In *ACM SIGCOMM Computer Communication Review*, volume 45, pages 213–226. ACM.
- Slavik, M., Mahgoub, I., and Alwakeel, M. (2015). Efficient multi-hop wireless broadcast protocol in vehicular networks using automated threshold function design. *International Journal of Communication Systems*, 28(12):1829–1846.
- Tao, S., Apostolopoulos, J., and Guérin, R. (2008). Real-time monitoring of video quality in ip networks. *IEEE/ACM Transactions on Networking (TON)*, 16(5):1052–1065.
- Torres, A., Calafate, C. T., Cano, J.-C., and Manzoni, P. (2015). Evaluation of flooding schemes for real-time video transmission in vanets. *Ad Hoc Networks*, 24:3–20.
- Ucar, S., Ergen, S. C., and Ozkasap, O. (2016). Multihop-cluster-based ieee 802.11 p and lte hybrid architecture for vanet safety message dissemination. *IEEE Transactions on Vehicular Technology*, 65(4):2621–2636.
- Video Sequences, N. R. L. (2016a). Videos used in the simulations ('truck accident') < URL <https://www.youtube.com/channel/UCUIJSLvBpeJbLAr6IsVXbJA/videos>>.
- Video Sequences, U. F. P. A. (2016b). Videos used in the QoE measurements ('truck accident') < URL <http://www.gercom.ufpa.br/sbrc2017-videoexperiments>>.
- Zaimi, I., Houssaini, Z. S., Boushaba, A., Oumsis, M., and Aboutajdine, D. (2016). Vehicular ad-hoc network: Evaluation of qos and qoe for multimedia application. In *International Conference on Networked Systems*, pages 367–371. Springer.